# Specific Heat Measurements of $Ba_{0.68}K_{0.32}Fe_2As_2$ Single Crystals: Evidence for a Multiband Strong-Coupling Superconducting State

P. Popovich,[1] A. V. Boris,[1,2] O. V. Dolgov,[1] A. A. Golubov,[3] D. L. Sun,[1] C. T. Lin,[1] R. K. Kremer,[1] and B. Keimer[1]

[1]*Max-Planck-Institut für Festkörperforschung, Heisenbergstrasse 1, D-70569 Stuttgart, Germany*

[2]*Department of Physics, Loughborough University, Loughborough, LE11 3TU, United Kingdom*

[3]*Faculty of Science and Technology and MESA+ Institute of Nanotechnology, 7500 AE Enschede, The Netherlands*

(Received 7 January 2010; published 7 July 2010)

The specific heat of high-purity $Ba_{0.68}K_{0.32}Fe_2As_2$ single crystals with the highest reported superconducting $T_c = 38.5$ K was studied. The electronic specific heat $C_p$ below $T_c$ shows two gap features, with $\Delta_1 \approx 11$ meV and $\Delta_2 \approx 3.5$ meV obtained from an $\alpha$-model analysis. The reduced gap value, $2\Delta^{\max}/k_B T_c \approx 6.6$, the magnitude of the specific-heat jump, $\Delta C_p(T_c)/T_c$, and its slope below $T_c$ exhibit a strong-coupling character. We also show that an Eliashberg model with two hole and two electron bands gives the correct values of $T_c$, the superconducting gaps, and the free-energy difference.

DOI: 10.1103/PhysRevLett.105.027003 PACS numbers: 74.25.Bt, 65.40.Ba, 74.20.Rp, 74.70.Xa

The newly discovered iron pnictide superconductors present an unusual case of multiband superconductivity in the vicinity of a magnetic instability. In view of the weak electron-phonon coupling in this class of superconductors [1], magnetic excitations are the most promising candidates for the pairing boson. The analysis of experimental data and the theoretical modeling of these systems are, however, considerably complicated by their complex electronic structure that involves at least four energy bands crossing the Fermi level. Despite intensive research, there is hence no consensus on the gap symmetry and on the nature of the pairing interaction.

The thermodynamic properties are a key source of surface-insensitive information on the electronic interactions and on the structure of the superconducting gap function. For a superconducting order parameter with alternating sign the pairing interactions are strongly influenced by impurity scattering, so that sample quality and phase purity issues are crucial for calorimetric experiments. Presumably because of such issues, the current specific-heat (SH) evidence of doped $BaFe_2As_2$ is still ambiguous. Recently two gaps were reported in electron-doped $Ba(Fe_{0.925}Co_{0.075})_2As_2$, supporting the results of nuclear magnetic resonance (NMR) and muon spin relaxation ($\mu$SR) studies [2]. In hole-doped $Ba_{1-x}K_xFe_2As_2$, on the other hand, prior SH experiments have shown only one gap with values of 6 meV in a single crystal with $T_c = 36.5$ K [3] and varying from 5.9 to 6.7 meV for $0.3 \leq x \leq 0.6$ (36.0 K $\leq T_c \leq$ 37.3 K) in polycrystalline specimens [4], in contrast to the observation of two nearly isotropic gaps in angle-resolved photoemission (ARPES) experiments [5]. Alas, all of the SH data thus far reported suffer from a residual low-temperature nonsuperconducting electronic contribution and show Schottky anomalies. In electron-doped $BaFe_2As_2$, this complication is likely due to structural defects caused by Co substitution directly in the superconducting FeAs planes. In hole-doped $BaFe_2As_2$, the substitution of Ba by K does not disturb the structure of the FeAs planes, but gives rise to electronic phase separation in the underdoped regime [6,7].

In this Letter we report a comprehensive study of the SH, $C_p$, of an optimally hole-doped, high-purity $Ba_{0.68}K_{0.32}Fe_2As_2$ single crystal with $T_c = 38.5$ K (onset), the highest transition temperature reported to date for this family of superconductors. The superconducting SH indicates two energy gaps with magnitudes $2\Delta_1 = 6.6k_BT_c$ and $2\Delta_2 = 2.2k_BT_c$, in agreement with the ARPES, $\mu$SR, and NMR results [5,8]. We also calculated the SH from the Eliashberg spectral function in a four-band spin-fluctuation model. From the solution of the Eliashberg equations we obtained the value of $T_c$, the superconducting gaps, and the temperature dependence of the free-energy difference in good agreement with the experimental data. The averaged electron-boson coupling constant, $\lambda^{\text{av}} \approx 1.9$, resulting from this analysis and consistent with the magnitude of the SH jump and its first derivative below $T_c$, is distinctly larger than the estimated electron-phonon coupling [1]. The strong coupling suggests the interaction with low-energy ($\lesssim$50 meV) interband spin fluctuations as the pairing mechanism.

The superconducting $Ba_{0.68}K_{0.32}Fe_2As_2$ and reference $Ba(Fe_{0.88}Mn_{0.12})_2As_2$ single crystals were grown from self-flux in zirconia crucibles sealed in quartz ampoules under argon atmosphere, as described earlier [9]. Their chemical compositions were determined by energy-dispersive x-ray spectrometry. The SH was measured in the temperature range between 2 and 200 K with a physical properties measurement system (Quantum Design) using the thermal relaxation technique. The measurements showed no difference between several cleaved pieces from the same batches. Bulk superconductivity in $Ba_{0.68}K_{0.32}Fe_2As_2$ was confirmed by magnetic susceptibility, dc, and infrared conductivity measurements, whereas $Ba(Fe_{0.88}Mn_{0.12})_2As_2$ did not show any signatures of superconducting or magnetic phase transitions.

 

Figure 1(a) displays unprocessed SH data on the $Ba_{0.68}K_{0.32}Fe_2As_2$ and $Ba(Fe_{0.88}Mn_{0.12})_2As_2$ single crystals. $C_p(T)/T$ of $Ba_{0.68}K_{0.32}Fe_2As_2$ shows no signs of low-temperature upturns or Schottky anomalies at any magnetic field. In the low-temperature limit [inset in Fig. 1(a)], the data can be fitted by $C(T)/T = \gamma(0) + \beta T^2$, where $\gamma(0)T$ represents the residual zero-temperature electronic SH and the second term the lattice SH. The fitting parameters for zero field are $\gamma(0) = 1.2(2)$ mJ/mol K$^2$ and $\beta = 0.496(1)$ mJ/mol K$^4$. For magnetic field $H = 9$ T we used the same $\beta$ and obtained $\gamma(0) = 6.4(2)$ mJ/mol K$^2$. These residual SH values are the lowest reported for FeAs-based superconductors so far, indicating the superior quality and high purity of our samples. The ratio of the residual electronic SH to its normal-state counterpart ($\gamma_K^N$, see below) yields an estimate of the nonsuperconducting phase fraction $\gamma(0)/\gamma_K^N \approx 1.2/50 = 2.4\%$.

Figure 1(b) highlights the superconductivity-induced jump anomaly of $C_p$, which exhibits the largest magnitude (125 mJ/mol K$^2$) and smallest width ($\leq$0.4 K) reported to date [2–4,10,11]. An external magnetic field applied perpendicular to the $ab$ plane gradually suppresses the jump and reduces the transition temperature by 1.4 K for $H = 9$ T. The transition temperature $T_c$ determined as the maximum of the derivative of $C_p(T)$ decreases linearly with magnetic field with a slope of $\delta H_{c2}(T)/\delta T|_{T_c} = -6.7$ T/K [Fig. 1(c)], which is consistent with the value reported in Ref. [10]. This is a factor of 2 larger than the value obtained from resistivity measurements on samples from the same batch [12]. This difference may be due to flux-flow effects.

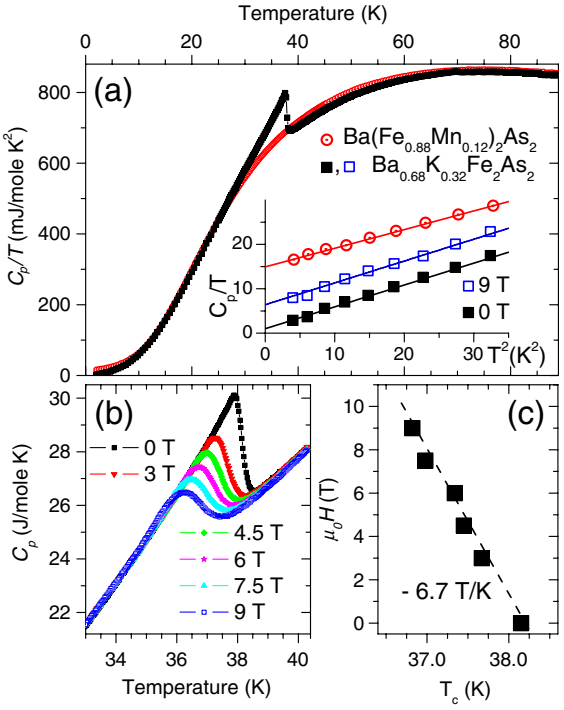


FIG. 1 (color online). (a) Temperature dependence of the specific heat $C_p/T$ of $Ba_{0.68}K_{0.32}Fe_2As_2$ (squares) and $Ba(Fe_{0.88}Mn_{0.12})_2As_2$ (circles). The inset shows a plot of $C_p/T$ vs $T^2$ at low $T$ for both samples. The lines represent the best fit to $C_p(T)/T = \gamma(0) + \beta T^2$. (b,c) Temperature dependence of $C_p$ of $Ba_{0.68}K_{0.32}Fe_2As_2$ near $T_c$ measured at different external magnetic fields applied perpendicular to the $ab$ plane.

In order to reliably extract the electronic contribution, $C_{\rm el}(T)$, from the total measured SH, the contribution of lattice excitations, $C_{\rm latt}(T)$, has to be accurately determined. The lattice SH of the parent compound $BaFe_2As_2$ cannot be accurately obtained because of the magnetic and structural phase transitions at $\sim$140 K. We found that substitution of 12% Fe by Mn suppresses the spin-density-wave state and does not induce superconductivity. The SH of $Ba(Fe_{0.88}Mn_{0.12})_2As_2$ [red circles in Fig. 1(a)] was found to be independent of magnetic field. The electronic and lattice SH heat terms extracted from a fit to low-temperature data on this compound [inset in Fig. 1(a)] are $\gamma(0) = \gamma_{\rm Mn}^N = 14.9(2)$ mJ/mol K$^2$ and $\beta_{\rm Mn} = 0.420(4)$ mJ/mol K$^4$, respectively. The lattice SH of $Ba(Fe_{0.88}Mn_{0.12})_2As_2$, $C_{\rm latt}^{\rm Mn}(T)$, was obtained by subtracting $\gamma_{\rm Mn}^N T$ from its total SH, $C_{\rm tot}^{\rm Mn}(T)$. The estimated Debye temperature is 306 K, somewhat higher than the corresponding value for superconducting $Ba_{0.68}K_{0.32}Fe_2As_2$ (277 K). Since the difference of the lattice parameters of both compounds does not exceed 1.5%, we assume that the phonon contributions to their SH and to the entropy obey a law of corresponding states. The normal-state SH of $Ba_{0.68}K_{0.32}Fe_2As_2$ can then be obtained from the commonly used corresponding states approximation [13]:

$$C_{\rm tot}^K(T) = C_{\rm latt}^K(T) + \gamma_K^N T = AC_{\rm latt}^{\rm Mn}(BT) + \gamma_K^N T, \quad (1)$$

where $\gamma_K^N$ is the Sommerfeld constant in the normal state of $Ba_{0.68}K_{0.32}Fe_2As_2$, and $A$ and $B$ are close to unity. From a least-squares fit of our data to Eq. (1) within the temperature range 40–150 K (more than 300 data points) under the constraint of entropy conservation, we obtained $\gamma_K^N = 50$ mJ/mol K$^2$, with $A = 0.95$ and $B = 1.03$. Figure 2 shows the difference, $\Delta C_{\rm el}(T)/T$, between measured $C_p(T)/T$ of $Ba_{0.68}K_{0.32}Fe_2As_2$ [Fig. 1(a)] and its normal-state counterpart $C_{\rm tot}^K(T)/T$ estimated from Eq. (1). The same $\Delta C_{\rm el}(T)/T$ (within the symbol size in Fig. 2) has also been obtained by representing the lattice contribution on a basis of Einstein modes [14]. The value of the Sommerfeld constant $\gamma_K^N = 50$ mJ/mol K$^2$ is in between those reported for the pristine end compounds $BaFe_2As_2$ (6.1 mJ/mol K$^2$ [15]) and $KFe_2As_2$ (69.1 mJ/mol K$^2$ [16]). This value exceeds the result of density functional theory (DFT) ($\gamma_{\rm DFT} \approx 10.1$ mJ/mol K$^2$ for $Ba_{0.6}K_{0.4}Fe_2As_2$ [17]) by almost a factor of 5, while it is consistently inferred from all SH experiments reported to date [3,4,11].

The thermodynamic critical field, $H_c(T)$, can be obtained from the free-energy difference between the normal and superconducting states $\Delta F(T) = \mu_0 V_m H_c^2(T)/2$, where $V_m = 6.05 \times 10^{-5}$ m$^3$/mol is the molar volume determined from our x-ray diffraction measurements on

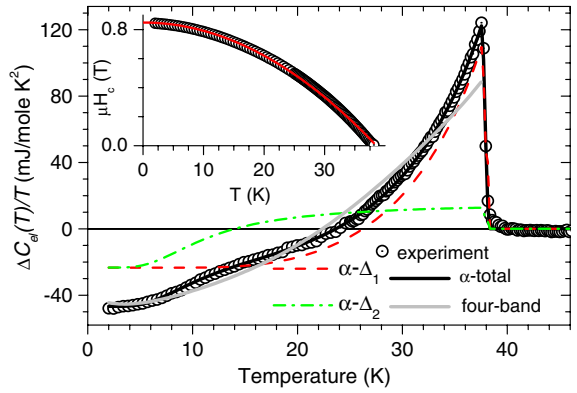


FIG. 2 (color online). Superconductivity-induced specific-heat difference of $Ba_{0.68}K_{0.32}Fe_2As_2$. The black solid curve is the result of a fit according to the two-gap $\alpha$ model. The dashed and dash-dotted curves represent the partial contributions of the two bands. The light gray line is the electronic specific heat calculated from the four-band Eliashberg model. Inset: Temperature dependence of the thermodynamic critical field (see text).

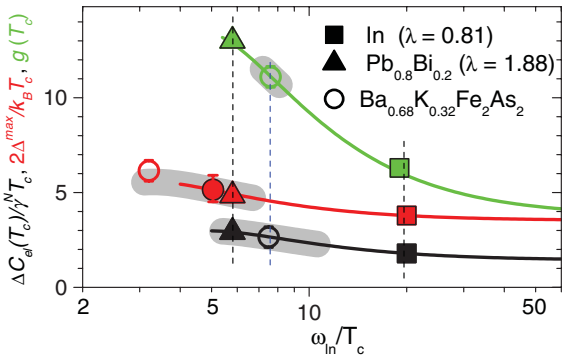


FIG. 3 (color). Comparison of the dimensionless superconducting jump, energy gap at $T = 0$, and slope of the specific heat near $T_c$ calculated by the semiphenomenological expressions in Ref. [19] (lines) with our results for $Ba_{0.68}K_{0.32}Fe_2As_2$ (open circles), and for $Pb_{0.8}Bi_{0.2}$ (triangles) and In (squares), after Ref. [19]. The open and solid circles represent the maximum gap values obtained by the two-band $\alpha$ and four-band Eliashberg model, respectively. Shaded areas represent the uncertainty in $\omega_{ln}/T_c$ according to the error bars in our data points.

$Ba_{0.68}K_{0.32}Fe_2As_2$. The temperature dependence of the thermodynamic critical field obtained by numerical integration of our data is displayed in the inset of Fig. 2. By fitting the thermodynamic critical field expressed as $H_c(T) = H_{c0}[1 - (T/T_c)^2]$ to our data between 2 and 38.5 K we obtained $\mu_0 H_{c0} = 0.85$ T, a value comparable to those of the cuprate superconductors [18].

In contrast to $\gamma_K^N$, the superconductivity-induced electronic SH is very sensitive to the sample quality and phase purity. We now show that if the impurity scattering is minimized, $\Delta C_{el}(T)$ reveals the intrinsic multigap strong-coupling nature of the superconducting state. Two quantities are commonly used to assess the pairing strength, namely, the reduced jump anomaly, $\Delta C_{el}(T_c)/(\gamma_K^N T_c)$, and the normalized slope of $\Delta C_{el}(T)$ right below $T_c$, $g(T_c) = -\partial[\Delta C_{el}(T)/(\gamma_K^N T_c)]/\partial T|_{T_c}$. Their magnitudes in $Ba_{0.68}K_{0.32}Fe_2As_2$, 2.5 and 11.1, respectively, are significantly larger than the corresponding BCS values of 1.43 and 3.77. In the framework of the Eliashberg formalism, the coupling strength can be expressed in terms of the ratio $\hbar\omega_{ln}/k_B T_c$, where $\omega_{ln}$ is the logarithmically averaged frequency of bosons mediating the Cooper pairing [19]. In Fig. 3, we place the reduced superconducting jump and $g$ value of $Ba_{0.68}K_{0.32}Fe_2As_2$ on a universal plot [19] as a function of this dimensionless coupling parameter. Both values correspond to $\hbar\omega_{ln}/k_B T_c = 7.5$, close to the prototypical strong-coupling superconductor $Pb_{0.8}Bi_{0.2}$. This comparison indicates strong-coupling superconductivity in $Ba_{0.68}K_{0.32}Fe_2As_2$.

The same issue can be addressed by considering the magnitude of the superconducting energy gap. Clearly, the prominent knee in the $\Delta C_{el}(T)/T$ data around $T = 15$ K (Fig. 2) cannot be described in terms of models with a single gap. We have hence fitted these data to the phenomenological multiband $\alpha$ model [20], which assumes a BCS temperature dependence of the gaps and has been widely used to analyze heat capacity data on $MgB_2$ [21]. The superconducting gap magnitudes at $T = 0$ are introduced as adjustable parameters $\alpha_j$, defined according to $\Delta_j(T) = (\alpha_j/\alpha_{BCS})\Delta_{BCS}$, where $\alpha_{BCS} = \Delta_{BCS}(0)/k_B T_c = 1.764$ is the weak-coupling value of the gap ratio. Another set of adjustable parameters is the fractions of the total electronic density of states, $\gamma_j/\gamma_K^N$, that each band contributes to the superconducting condensate. Figure 2 shows the result of our multigap fit (black solid curve) with only two gaps survived, $\alpha_1 = 3.3$, $\alpha_2 = 1.1$, and $\gamma_1 \sim \gamma_2 \sim 0.5\gamma_K^N$, which reproduces well $\Delta C_{el}(T)/T$ below $T_c$. One of the gaps, $\Delta_2(0) = 3.5$ meV, is somewhat smaller than $\Delta_{BCS}(0)$, whereas the other one, $\Delta_1(0) = 11$ meV, is much larger. Our analysis thus yields thermodynamic evidence of two different superconducting gaps (or groups of gaps) with quite different absolute values in $Ba_{0.68}K_{0.32}Fe_2As_2$, in agreement with ARPES and $\mu$SR results [5]. Further, marking the corresponding point, $2\Delta^{max}/k_B T_c = 6.6$, on the universal plot of Fig. 3 strongly supports our conclusion about the strong-coupling nature of superconductivity in this compound.

Finally, we show that the strong-coupling scenario can be described by fully microscopic calculations in the framework of a spin-fluctuation model. Such models generically yield $s$-wave superconducting gaps with different signs on different bands ("$s_\pm$ state") [22]. It was shown in Ref. [23] that strong-coupling effects lead to merging of the gaps in a simple two-band $s_\pm$ model. Therefore, a more realistic four-band model based on a band structure with two hole bands and two electron bands crossing the Fermi level needs to be considered [24]. The main input into the Eliashberg equations is the spectral function of the intermediate bosons. Following Ref. [25] we took a spin-fluctuation coupling function $\tilde{B}_{ij}(\Omega) = \lambda_{ij} B(\Omega)$ [inset of Fig. 4] with a linear $\Omega$ dependence at low frequencies, a

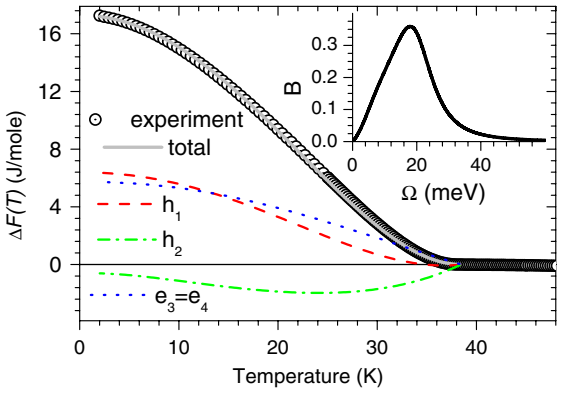


FIG. 4 (color online). Free-energy difference between normal and superconducting states, experimentally obtained (open circles) and calculated from the four-band Eliashberg model (light gray solid line). The dashed, dash-dotted, and dotted lines represent the partial contributions of the individual bands. Inset: Spin-fluctuation coupling function $B(\Omega)$.

maximum at $\hbar\Omega_{\mathrm{SF}}^{\max} = 18$ meV, and a fast decay at $\Omega > \hbar\Omega_{\mathrm{SF}}^{\max}$, in qualitative agreement with recent experimental data on the normal-state dynamical spin susceptibility of $Ba(Fe_{1-x}Co_x)_2As_2$ [26,27]. Here $\lambda_{ij}$ is the coupling constant for pairing of electrons in bands $i$ and $j$. For our calculations we use the intraband coupling matrix elements $\lambda_{ii} = 0.2$ in order to take account of the weak electron-phonon contribution [1], for interband repulsion $\lambda_{12} = \lambda_{34} = 0$ due to the symmetry of the wave functions, and $\lambda_{13} = \lambda_{14} = -1.0$, $\lambda_{23} = \lambda_{24} = -0.2$ [$\lambda_{ji} = \lambda_{ij} N_i^{h,e}(0)/N_j^{h,e}(0)$]. The corresponding densities of states are taken as $N_1^h(0) = 29\ \mathrm{Ry}^{-1}$, $N_2^h(0) = 43\ \mathrm{Ry}^{-1}$ for the hole bands, and as $N_3^e(0) = N_4^e(0) = 8.5\ \mathrm{Ry}^{-1}$ for the two equivalent electron bands [14]. The chosen parameters, $\lambda_{ij}(i \neq j)$ and $N_i^{h,e}(0)$, allow the best simultaneous fit to the experimental values of $T_c$, the superconducting gaps, and the temperature dependence of the free-energy difference, yielding $T_c = 38.5$ K, and the following gap values: $\Delta_1^h = -8.5$ meV, $\Delta_2^h = -3.6$ meV for hole bands, and $\Delta_3^e = \Delta_4^e = 9.2$ meV for electronic ones. The effective coupling constant averaged over all bands, $\lambda^{\mathrm{av}} = \sum_{ij} N_i^{h,e}(0)\lambda_{ij}/N_{\mathrm{tot}}$, has a value of 1.9, remarkably close to the coupling constant reported for $Pb_{0.8}Bi_{0.2}$ [19] and in agreement with the conclusions of our phenomenological analysis presented in Fig. 3. The consistency with the experiment tolerates some variation of the parameters and remains satisfactory for $\hbar\Omega_{\mathrm{SF}}^{\max}$ within the 10–20 meV energy range [14]. A shift of $\hbar\Omega_{\mathrm{SF}}^{\max}$ to lower energy leads to larger values of $\lambda^{\mathrm{av}}$ with $N_i^{h,e}(0)$ approaching the results of DFT [17]. This accounts for the strong renormalization of the Sommerfeld constant $\gamma_K^N/\gamma_{\mathrm{DFT}} \sim 5$.

The superconductivity-induced free-energy difference, $\Delta F(T)$, was calculated by using the expressions in Ref. [21]. The result is presented in Fig. 4, along with the partial band contributions to $\Delta F(T)$ which demonstrate that the superconductivity in the second hole band has an induced origin. Figure 4 also shows that the result of the model calculation is in fairly good agreement with the free-energy difference obtained by integrating the experimentally measured $\Delta C_{\mathrm{el}}(T)$, while some deviations between the calculated and observed SH can be seen in Fig. 2. Some such deviations are expected because feedback effects of superconductivity on the bosonic spectral function, which lead to the formation of a temperature-dependent "resonant mode" in the spin-fluctuation spectrum below $T_c$ [26], have not been considered in the calculations.

We thank L. Boeri and A. N. Yaresko for helpful discussion and G. Siegle for experimental assistance. We acknowledge support by the Deutsche Forschungsgemeinschaft (DFG) via Grant No. BO 3537/1-1 in SPP 1458.

[1] L. Boeri, O. V. Dolgov, and A. A. Golubov, Phys. Rev. Lett. **101**, 026403 (2008).
[2] F. Hardy *et al.*, Phys. Rev. B **81**, 060501(R) (2010).
[3] G. Mu *et al.*, Phys. Rev. B **79**, 174501 (2009).
[4] C. Kant *et al.*, Phys. Rev. B **81**, 014529 (2010).
[5] D. V. Evtushinsky *et al.*, Phys. Rev. B **79**, 054517 (2009).
[6] J. T. Park *et al.*, Phys. Rev. Lett. **102**, 117006 (2009).
[7] D. S. Inosov *et al.*, Phys. Rev. B **79**, 224503 (2009).
[8] K. Matano *et al.*, Europhys. Lett. **87**, 27 012 (2009).
[9] G. L. Sun *et al.*, arXiv:0901.2728.
[10] U. Welp *et al.*, Phys. Rev. B **79**, 094505 (2009).
[11] J. G. Storay *et al.*, arXiv:1001.0474.
[12] D. L. Sun, Y. Liu, and C. T. Lin, Phys. Rev. B **80**, 144515 (2009).
[13] J. W. Stout and E. Catalano, J. Chem. Phys. **23**, 2013 (1955).
[14] See supplementary material at http://link.aps.org/supplemental/10.1103/PhysRevLett.105.027003 for specific details of the data analysis.
[15] A. S. Sefat *et al.*, Phys. Rev. B **79**, 094508 (2009).
[16] H. Fukazawa *et al.*, J. Phys. Soc. Jpn. **78**, 083 712 (2009).
[17] A. N. Yaresko (private communication).
[18] W. Y. Liang and J. W. Loram, Physica (Amsterdam) **404C**, 230 (2004).
[19] J. P. Carbotte, Rev. Mod. Phys. **62**, 1027 (1990). See expressions (4.1) and (5.9), and (5.10) and Figs. 31, 53, 54.
[20] H. Padamsee, J. E. Neighbor, and C. A. Shifman, J. Low Temp. Phys. **12**, 387 (1973).
[21] A. A. Golubov *et al.*, J. Phys. Condens. Matter **14**, 1353 (2002); O. V. Dolgov *et al.*, Phys. Rev. B **72**, 024504 (2005).
[22] I. I. Mazin *et al.*, Phys. Rev. Lett. **101**, 057003 (2008).
[23] O. V. Dolgov and A. A. Golubov, Phys. Rev. B **77**, 214526 (2008); O. V. Dolgov *et al.*, Phys. Rev. B **79**, 060502(R) (2009).
[24] L. Benfatto, E. Cappelluti, and C. Castellani, Phys. Rev. B **80**, 214522 (2009); G. A. Ummarino *et al.*, Phys. Rev. B **80**, 172503 (2009).
[25] D. Parker *et al.*, Phys. Rev. B **78**, 134524 (2008).
[26] D. S. Inosov *et al.*, Nature Phys. **6**, 178 (2010).
[27] C. Lester *et al.*, Phys. Rev. B **81**, 064505 (2010).